Frontiers in Scientific Research and Technology

Online ISSN: 2682-297
Print ISSN: 2682-2962
http://fsrt.journals.ekb.eg

FSRT J 5 (2023) 73 - 83 10.21608/FSRT.2023.178854.1078

Lithostratigraphy, Stable Isotope Stratigraphy and Calcareous Nannofossils Biostratigraphy of the Danian-Thanetian at Nukhul, Sinai, Egypt

Atef M. Kasem

Geology Department, Faculty of Science, Damanhour University, Damanhour, Egypt

ARTICLE INFO

Article history:
Received 5 December 2022
Received in revised form 6 January 2023
Accepted 7 January 2023
Available online 10 January 2023

Keywords
Nukhul,
Calcareous Nannofossils,
Danian,
Selandian,
Carbon Isotopes.

ABSTRACT

Paleocene sediments exposed at Nukhul, Sinai, Egypt were subjected to a detailed calcareous nannofossil biostratigraphy besides tracking changes in carbonate contents, $\delta^{13}C$ and $\delta^{18}O$ values. This Paleocene outcrop extends through the Dakhla - Tarawan formations. About 8.5 m of Dakhla F. consists of grey calcareous shale, and 2 m from the Tarawan F. consists of yellowish argillaceous limestone were investigated. Five calcareous nannofossil zones (NP2/3 - NP7/8) were delineated. The Late Danian Event was traced at a level characterized by an abrupt decrease in carbonate content and $\delta^{18}O$ values, and minimum values of calcareous nannofossil's diversity and abundance that support warming conditions during this interval. The Danian/Selandian contact was placed in coincidence with the base of Zone NP5. No remarkable changes in lithology or in $\delta^{13}C$ and $\delta^{18}O$ values were noted close to this boundary except an abrupt drop in $\delta^{18}O$ values just below it and increase in $\delta^{13}C$ values slightly above this level. A distinct drop in carbonate content and calcareous nannofossil diversity was documented close to this boundary indicating warming episode. Calcareous nannofossils indicate a hiatus within Danian at Nukhul. The Selandian/Thanetian boundary was placed in coincidence with the base of NP7/8 combined Zone. No remarkable change in lithology, calcareous nannofossil assemblage, or $\delta^{13}C$ and $\delta^{18}O$ values were recorded across this boundary except the sudden drops in $\delta^{13}C$ and $\delta^{18}O$ values slightly below and above it. Calcareous nannofossils, $\delta^{13}C$ and $\delta^{18}O$ data reflect an upward increase in paleotemperature throughout the Paleocene at Nukhul.

1. Introduction

Paleocene Series was formally divided into three Stages (Danian, Selandian, plus Thanetian, Jenkins and Luterbacher 1992). The base of Selandian Stage's Global Stratotype Section and Point (GSSP) were chosen at Zumaia in northern Spain (Schmitz et al., 2011). During Paleocene, short-lived warming episodes were encountered that resulted sedimentological, paleontological, geochemical and climatic variations (Thomas et al., 1999; Speijer, 2003a, b; Arenillas et al., 2008; Quillévéré et al., 2008; Sprong et al., 2011, 2012, 2013; Schmitz et al., 2011; Dinarès-Turell et al., 2012; Monechi et al., 2013; Kasem et al., 2017; Faris et al., 2018; Kasem et al., 2022). These events include Danian ⁄Selandian (D/S) transition (Schmitz et al., 2011), and the Mid Paleocene Biotic Event (MPBE) (Bernaola et al., 2007).

These warming episodes had been characterized by drops in carbon isotope excursions (CIEs) and the level of carbonate, as well as variations in calcareous nannofossil assemblages (Dupuis et al., 2003; Aubry et al., 2007; Bernaola et al., 2007; Schmitz et al., 2011; Soliman et al., 2014; Karoui-Yaakoub et al., 2016**,** Kasem et al., 2017; Faris et al., 2018, and Abu Shama et al., 2020)**.** The negative $\delta^{13}C$ excursions are usually interpreted as a response to increase in paleotemperature (Bornemann, 2003), possibly a carbon reservoir added more ^{13}C to the water and atmosphere (Dickens et al. 1997). These variations caused an increase in atmospheric CO_2 and temperature, as well as making the calcite compensation depth (CCD) shallower (Zachos *et al*. 2005; Coccioni et al., 2010).

At Zumaia, the Danian/Selandian limit is marked by a lithological change from the Aitzgorri F. that is limestone-dominated to the Itzurun F., which consists of marls. Moreover, it was marked by the ending of blooming of *Braarudosphaera bigelowii* close to the base of calcareous nannofossil Zone NP5 (Schmitz et al., 2011). The start of Thanetian at Zumaia was delineated relative to the MPBE (Schmitz et al., 2011).

The Paleocene sequences in Egypt have detailed records for tracking biologic and isotopic variations

* Corresponding author at Damanhour University

E-mail addresses: Kasematef@yahoo.com (Atef M. Kasem)

throughout the Danian-Thanetian. Therefore, several Paleocene successions had received biostratigraphic studies based on calcareous nannofossil assemblages (Dupuis et al., 2003; Kasem et al., 2017, 2022, more references therein). Faris and Salem (2007) studied the Paleocene-lower Eocene at Nukhul (Sinai, Egypt) in terms of calcareous nannofossils. They placed the D/S boundary by the LO of *Fasciculithus* taxa. They recorded a hiatus at the S/T boundary at the Gabal Nukhul.

The essential targets of this study include implementation of calcareous nannofossil biozonation and denoting the stage boundaries of the study interval, track variations in calcareous nannofossils, $\delta^{13}C$ and $\delta^{18}O$ data, carbonate contents and shed some light on the climatic changes throughout the Danian-Thanetian.

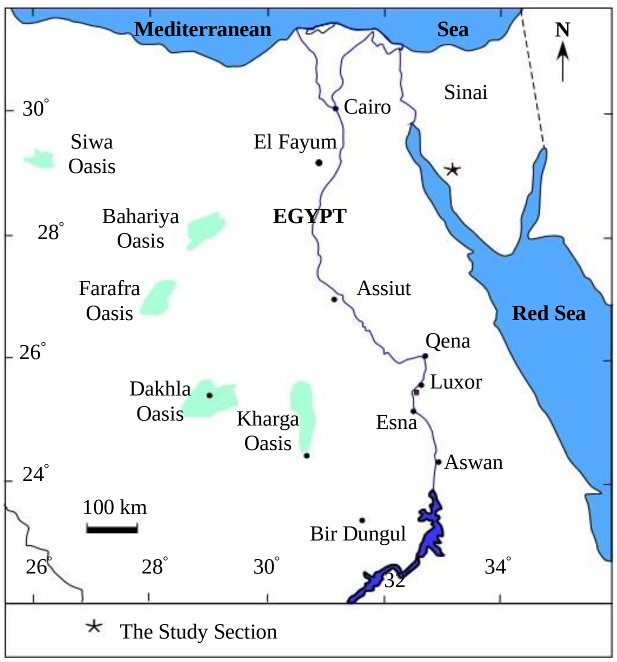

Fig. 1: A map shows the position of the Nukhul section

2. Materials and Methods

Forty nine rock samples were examined from Paleocene at Nukhul, West Central Sinai (Fig. 1). For calcareous nannofossil examination, about 0.1gm of dry sediment had been dissolved in 10 ml of distilled water and a 0.25 mm of the solution was placed on a 22x22mm coverslip, which was dried on a hot-plate and mounted on a slide by D.P.X mountant. Species were counted in definite fields of view (ranges form 27-65 FOVs) and relative abundances were recognized (Kasem et al., 2022). The slides were investigated at 1250X magnification by Euromex Iscope microscope. Oxygen as well as carbon isotopes had been measured by Finnigan-MAT 252 spectrometer at University of Florida. Inorganic carbon was measured at Stable Isotope Mass Spectrometer Laboratory at University of Florida, USA.

3. Geologic setting and lithostratigraphy

3.1. Geologic setting

Sinai is bounded by African, Arabian Peninsula and Mediterranean Sea from the west, east, and north, respectively. The study section locates at the southern flank of Wadi Nukhul, West Central Sinai. It is situated at Latitude 29°04'46"N and Longitude 33° 10'21"E. The study interval belongs to Paleocene. A geographic map of Egypt during the late Paleocene is provided below showing the various rock facies types in the study area (Fig. 2, after Guiraud and Bosworth, 1999).

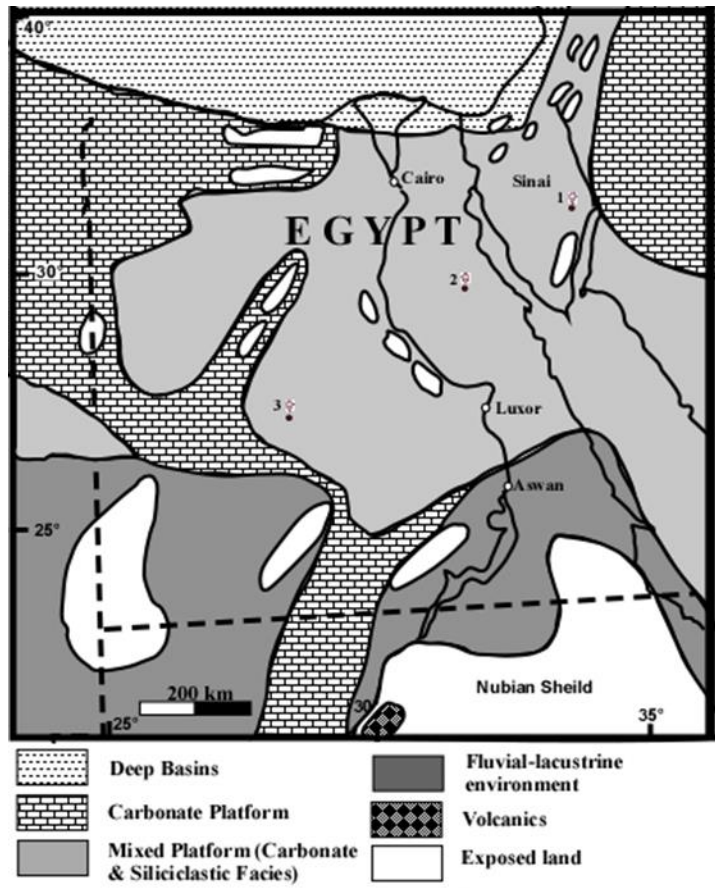

Fig. 2: A paleogeographic map of Egypt during the late Paleocene modified after Guiraud and Bosworth (1999).

3.2. Lithostratigraphy

The study interval that outcrops at Nukhul extends through the Dakhla - Tarawan formations.

a- The Dakhla Formation

The Dakhla Formation's type section crops out north of Mut, Dakhla Oasis (Said, 1961). It is 225 m of marls, shales, as well as clays intercalated with calcareous beds rich in sands and silts underlie the Tarawan F. and overlie the Duwi F. (Awad and Ghobrial, 1965). The included part of Dakhla F. at Nukhul is about 8.5 m of grey calcareous shale and is assigned to age Danian–Thanetian (Fig. 3).

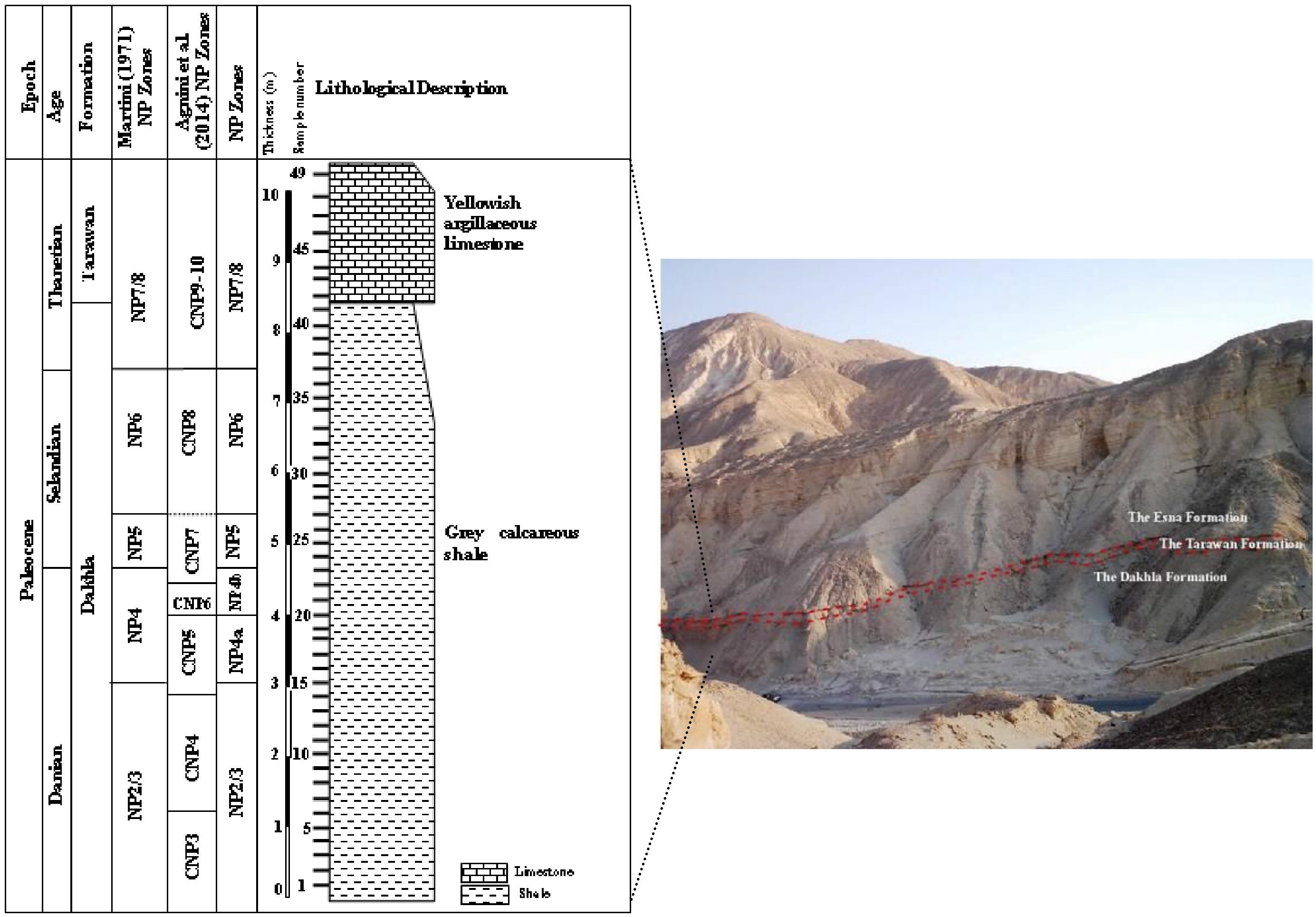

Fig. 3: Stratigraphic columnar section of the Danian-Thanetian interval at Nukhul, Sinai, Egypt and a field photograph shows panoramic view of the study interval.

b- The Tarawan Formation

The type locality of the Tarawan F. was hosted by Gabal Tarawan at Kharga Oasis, Western Desert (Awad and Ghobrial, 1965). This formation consists of fossiliferous, argillaceous limestone at G. Tarawan. This formation is marly in its lower portion, intercalated with shale and clay beds and grades into chalky limestone and siliceous limestone (Awad and Ghobrial, 1965). About two meters from the bottom of this formation has been probed and is consisting of yellowish argillaceous limestone. Calcareous nannofossil data reveal that this formation conformably overlies the Dakhla F.. This formation belongs to the Thanetian Age (Fig. 3).

4. Calcareous Nannofossil Biostratigraphy

Variations in calcareous nannofossil assemblages are helpful tool for biozonation and world-wide correlation of Cenozoic deposits (Romein, 1979; Varol, 1989; Agnini et al., 2014; 2017). Paleocene Zonation Scheme suggested by Martini (1971) was applied in this study with a slight modification, and Romein's (1979) conclusion of gathering Zone NP2 plus NP3 and Zone NP7 plus Zone NP8 was adopted. Abbreviations in this manuscript include LO (Lowest Occurrence), when the first specimen appears; LCtO (lowest continuous occurrence), where the occurrence is scarce; however stratigraphic range became continued; LCO (lowest common occurrence); where the species became common; and HO for "Highest Occurrence", where the taxon vanishes. The stratigraphic distributions of the taxa recognized and their counts are shown in the table. Microphotographs of some taxa are shown on plates 1 and 2. Five zones were set apart covering the study interval. These biozones are discussed below.

4.1 Cruciplacolithus tenuis Zone (NP2/3, and extends from the LO of *Cruciplacolithus tenuis* to the LO of *Ellipsolithus macellus* (Romein, 1979). There are disputes concerning the distinction of *C. danicus, C. edwardsii, C. asymmetricus*, and *C. consuetus* (Brotzen, 1959; Van Heck and Prins, 1987, and Romein, 1979). As a result, it was suggested to exclude *C. danicus* from being a reliable zonal marker (Romein, 1979 and this study). This zone covers about 3 m from the lower part of Dakhla F. at Nukhul (Fig. 3), and is assigned to the Danian Age.

4.2. Ellipsolithus macellus Zone (NP4, and spans from the LO of *Ellipsolithus macellus* to the LO of *Fasciculithus* *tympaniformis,* Martini, 1971). It is ~ 1.7 m thick at Nukhul (Fig. 3). Discontinuous range of *E. macellus* probably resulted from diagenesis and/or dissolution (Table). Varol (1989) subdivided the interval that is equivalent to the NP4 Zone into several zones and subzones, however, this subdivision cannot be fully applied in this study. Later, *E. macellus* Zone had been subdivided into NP4a plus NP4b Subzones based on the LO of *Sphenolithus primus* (Quillévéré et al., 2002). In 2014, Agnini et al. used the LO of *S. moriformis* group, which includes *S. primus* and *S. moriformis*, to delineate the start of Zone CNP6. However, discrepancies were documented relative to the LOs of *S. primus* (Bernaola et al. 2009) and this species is scarce and discontionous in the bottom of its stratigraphic range (Schmitz et al. 2011, and Monechi et al. 2013). Thus, the LCtO of *S. primus* was used as marker for biostratigraphic studies (Quillevere et al. 2002, and Monechi et al. 2013). The LCtO of *S. primus* is at 5.8 m above its LO, and below the boundary between the Danian and Selandian at Zumaia (Bernaola et al., 2009), however, *S. primus* was observed ~2.5 m overhead of the Selandian's base at the Egyptian Qreiya section (Schmitz et al. 2011). In this study, *S. primus* continuously occurs just above the LO of *Lithoptychius schmitzii*, the only representative of the first radiation of *Fasciculithus* recorded at Nukhul (Table).

Table: Abundance of the Danian-Thanetian coccoliths at Nukhul, Sinai, Egypt (Continued)

Epoch	Age	Formation	Nannofossil Zones	Sample Number	Abundance	Abundnce per FOV	Diversity	Zeugrhabdotus sigmoides	Micula decussata	Micula murus	Watznaueria barnesiae	Micula concava	Prediscosphaera cretacea	Gorkaea pseudanthophorus	Micula prinsii	Retecapsa crenulata	Cribrosphaerella ehrenbergii	Eiffellithus turriseiffelii	Cylindralithus sculptus	Chiastozygus amphipons	Tetrapodorhabdus decorus	Lithraphidites carniolensis	Ahmuellerella octoradiata	Schyphosphaera sp.	Eiffellithus turriseiffelii	Microrhabdulus decoratus	Eiffellithus parallelus	Watznaueria biporta	Micula swastica	Braarudosphaera bigelowii	Micula prinsii	Thoracosphaera operculata	Thoracosphaera saxea	Ericsonia subpertusa	Coccolithus pelagicus	Ericsonia robusta	Thoracosphaera heimii	Cruciplacolithus primus	Cruciplacolithus intermedius	Cruciplacolithus edwardsii	Arkhangelskiella cymbiformis	Chiasmolithus danicus	Prinsius martinii	Prinsius bisulcus	Prinsius sp.	Cruciplacolithus tenuis
Paleocene	Thanetian	Tarawan	NP7/8	48	249	5.3	9																											A	4	F								F		F
				47	369	8.2	11	F																										A	C	F										F
				46	321	12	16	F																										A	C	C										C
				45	323	9.8	17																											A	C	C									F	F
				44	243	6.1	15																											A	C	C									F	F
				43	320	8	15	F																										A	C	C										C
				42	158	3.2	12	F																								R		C	R											R
		Dakhla		41	180	3.6	9																									F		C	C	R										R
				40	214	4.3	10	F																								R		A	F											
				39	290	4.8	21	F																						R				A	F	R						R				R
				38	272	6.8	16	F																										A	C	F										F
				37	291	8.8	17	C																										A	C	C										F
	Selandian		NP6	36	146	4.2	13	F																										A	F									F		F
				35	252	5.6	20	C																								F		A	C	F								C	F	F
				34	259	7.4	24	C																										A	C	F									F	F
				33	300	7.5	18	C																										A	C	C								F		
				32	278	7	18	C																										A	C	F								F		F
				31	287	8.2	22	C																										A	C	C						F			F	F
				30	251	8.4	18	C																										A	C	C								F		F
				29	228	7.6	20	C																										A	C	F								F		F
				28	221	4.4	23	C																										A	C	C		F				F		F	F	
				27	298	7.5	24	C																								F		A	C	F			F			F			F	C
			NP5	26	206	4.1	21	F																								F		A	C	C							F	F		F
				25	220	6.3	22	6																						F				A	C	C						F			F	C
				24	234	5.9	17	C																										A	C	F			F					F	F	C
				23	220	4.9	25	F			F																					C		A	C	F		F	F						F	C
				22	161	2.7	22	F																								C		A	C			F	F					F		F
	Danian		NP4	21	57	1	13	F																F								C		C	F	F			F					F		F
				20	167	3.8	16	C			F								F													C		A	C	C		F	C	F		F				C
				19	36	0.6	10	F																								F		C	F	F		R	F							
				18	153	3.4	17	F			F															F						C		A	C	C	F	F	F			F			F	F
				17	122	2.6	15	F																						F		F	F	A	C	C	C	F	F	F		F			F	F
				16	104	2.6	12	F			F																					C		A	C	C	F		C							F
				15	192	4.8	17	C			F													F								C	F	A	C	C	F	F	C			F				F
			NP2/3	14	244	7	13	F			F																					C		A	A	C	F	F	C		F	F				
				13	252	5.9	11	F			4																					C		A	A	C	F	F	C			F				
				12	201	4.2	11	C			F																					C	F	A	C	C		F	C			F				
				11	124	3.9	14	C	F		F														F							C	F	A	C	C	C	F	C		F	F				
				10	225	6.4	20	C	F	F	F	F			F		F											F				C	F	A	C	A	C	F	F		F	F	F			
				9	250	6.6	23	C	C	F	F	F	F				F					F			F		F	F	F			C	F	A	C	C	C	F	F		F	F	F			
				8	154	4.4	18	C	C		C			F			F			F		F			F							C		A	C	F		F	F		C		F			
				7	197	4.9	19	C	C		F	F	F							F	F	F										C	F	A	C	C		F	C		C	F	C			
				6	215	6.1	23	C	C		9	F		F			F			F					F	F	F	F			F	C	F	A	C	C		F	C		C	C	F			F
				5	119	3	17		F		F		F				F		F	F	F	F			F							C		C	C	C		F	C		F	F				
				4	202	6.7	21	C	C		C	F					F		C	F		F			F	F		F				A	F	A	A	C		F	C	F	C	F				
				3	217	6.2	18	C	C		C	F	F				F			F		F			F	F						A		C	A	C		F	C		C				C	
				2	126	3.6	20	C	C		C		F	F			F				F	F			F	F						C		C	C	C		F	C	F	F	F			F	
				1	162	4	27	C	C	F	C	F	6	F	F	F	3	F	F	F	F	F	F	F	F	F						C	F	C	F	F		F	C		F		?			

Table: Abundance of the Danian-Thanetian coccoliths at Nukhul, Sinai, Egypt

Epoch	Age	Formation	Nannofossil Zones	Sample Number	Lanternithus simplex	Neochiastozygus perfectus	Markalius inversus	Ellipsolithus macellus	Neococcolithes protenus	Prinsius dimorphosus	Toweius pertusus	Cruciplacolithus edwardsii	Neochiastozygus modestus	Bomolithus megastypus	Lithoptychus schmitzi	Octolithus sp.	Sphenolithus primus	Chiasmolithus edentulus	Lithoptychius ulii	Bomolithus elegans	Lithoptychius stegastus	Sphenolithus anarrhopus	Lithoptychius janii	Fasciculithus clinatus	Fasciculithus tympaniformis	Lithoptychius billii	Neochiastozygus junctus	Fasciculithus involutus	Chiasmolithus consuetus	Fasciculithus richardii	Chiasmolithus grandis	Neochiastozygus distentus	Chiasmolithus bidens	Toweius eminens	Heliolithus kleinpellii	Bomolithus conicus	Cruciplacolithus frequens	Lithoptychius pileatus	Toweius tovae	Zygrhablithus bijugatus	Coronocyclus nitescens	Neococcolithes protenus	Discoaster mohleri	Discoaster lenticularis	Pontosphaera exilis	Discoaster falcatus	Discoaster nobilis
Paleocene	Thanetian	Tarawan	NP7/8	48		F					5						C								C																						
				47		F		F			F						A								A																		F				
				46		C					F						A								A	F			F				F				F				F		F	F			
				45		C		F			C		F				A		F						A							F	F								F		F				F
				44		F		F			C		F				A							F	C									F			F						F				
				43		C		F			F						A								C				F														F	F		F	F
				42		R					R						A					F		R	C			R																			
		Dakkhla		41							F						A							R	C																						
				40		F							R				A								C								R										R				
				39		F		R			C						A						R	R	C			R	R				R		R			R					F		R		
				38		F		F			F						A			F			F	F	A			1							F								F				
				37		F		F			F		F	F			A	F			F			F	A										C								F				
	Selandian		NP6	36		F					C		F				C				F		F		C	F									C												
				35		F					C		F	F			C			F	F		F	F	A									F	C												
				34		C					C		F				C	F		F			F	F	C	F			F			F	F	F	C		F		F			F					
				33		F					C			F			C			F					C							F		F	C		F	F	F			F					
				32		F					C		F				A			F					C			F				F	F		C		F	F					?				
				31							C			F			C			F	F				C	F		F	F		F	F			F		F			F	F						
				30		F					C			F			C			F	F				C	F				F					C		F		F								
				29		F					C			F			A			F			F		C	F		F		F		F			C		C	F									
				28		F		F			C						C			F	F		F		C	F			F	F		F		F	C		F										
				27		F					C		F				C			F			F	F	C	F		F				F	F	F	F	F											
			NP5	26		R					C		R				C	R	R	R			R	F	C	R						R	R														
				25		F		F			C						C		F	F	F			F	C	C		F	F	F	F																
				24		F					F		F			F	C			F					C	F		F																			
				23		C					C		F			F	C	F	F	F	F		C	F	C	F	F	F																			
				22		F		F			F				F	F	C	F	F	F	F	F	C	F	C																						
	Danian		NP4	21		C										F	C	F																													
				20		C		F								F	C	F																													
				19		R		R							R																																
				18				F	F				F	F																																	
				17		F																																									
				16		F		F				F																																			
				15		F		F		F		F																																			
			NP2/3	14	F	F					?																																				
				13		F																																									
				12		F																																									
				11																																											
				10						F																																					
				9																																											
				8			F		F																																						
				7	F	?																																									
				6																																											
				5																																											
				4																																											
				3																																											
				F																																											
				F																																											

Abundance
VA; Verry Abundant (>10 Specimen/ field of view)
A; Abundant (1-10 Specimen/field of view)
C; Common (1 Specimen / 1-10 feild of view)
F; Few (1 Specimen / 11-50 field of view)

***4.3. Fasciculithus tympaniformis* Zone** (NP5, extends from the LO of *Fasciculithus tympaniformis* to the LO of *Heliolithus kleinpellii* (Hay et al., 1967). The LO of *F. tympaniformis* was used to delineate the base of Martini's (1971) Zone NP5, Okada and Bukry's (1980) Zone CP4; Romein's (1979) *Fasciculithus tympaniformis* Zone and Varol's (1989) Zone NTp9. *Fasciculithus tympaniformis* Zone covers ~0.8 m within the Dakhla F. at Nukhul (Fig. 3).

***4.4 Heliolithus kleinpellii* Zone** (NP6, extends from the LO of *Heliolithus kleinpellii* to the LO of *Discoaster mohleri*, Hay et al., 1967). It is about 2 m thick at Nukhul (Fig. 3, Table) and is appointed to Thanetian Age. The biostratigraphic significance of the LO of *H. kleinpellii* was disputed where intermediate forms between *H. kleinpellii* and *H. cantabriae* were recorded (Agnini et al. 2007). Therefore, the LO of *H. kleinpellii* has to be utilized as a zonal marker with caution. Several Egyptian sections have a minor hiatus at the S/T indicated by the absence of Zone NP6 (e. g. Tantawy, 1998, and Faris and Salem, 2007). *Heliolithus kleinpellii* disappears in the basal part of Zone NP7/8 (Table).

***4.5. Discoaster mohleri* Zone** (NP7/8, spans the interval between the LOs of *Discoaster mohleri* and *D. multiradiatus*, Romein, 1979). *Discoaster mohleri* was considered a reliable bioevent (Martini, 1971, and Agnini et al., 2014, 2017). However, *Heliolithus riedelii* is not a reliable zonal marker (Romein, 1979; Varol, 1989; Agnini et al., 2007b). Consequently, it was excluded from being reliable marker (Romein, 1979). Bukry (1973) had used *Discoaster nobilis* in place of *Heliolithus riedelii*, but *D. nobilis* was recorded in coincidence with the first occurence of *D. multiradiatus* (Romein, 1979). This zone was restricted to the Tarawan F. in various egyptian sections (Tantawy, 1998, and Kasem et al 2017), however, this combined zone extends from the uppermost Dakhla F. across the Tarawan F. at Nukhul (Fig. 3).

5. $\delta^{13}C$, $\delta^{18}O$ and carbonate contents

The $\delta^{13}C$ and $\delta^{18}O$ isotopic variations depend on the water's isotope composition and temperature (Stassen et al., 2009). Thus, they provide a widely used tool for tracking climatic changes (Shaaban, 1997). At the Zumaia section, the bulk $\delta^{13}C$ data show two remarkable negative CIEs: the first is smaller (~0.5‰) that was correlated with the LDE, which is about 11 m beneath the Selandian's base (Westerhold et al., 2008, and Sprong et al., 2013). The second $\delta^{13}C$ excursion (~1 ‰) was recorded shortly above the base of *Zone NP5* (Westerhold et al., 2011). At Nukhul, no remarkable variations or in carbonate contents mark the LDE or D/S boundary (Fig. 4). Moreover, no distinct changes in $\delta^{13}C$ and $\delta^{18}O$ values were recorded close to the basis of Zone NP5 (sample 22) except the sudden decrease in $\delta^{18}O$ values in samples number 18, 19 and 21 into -5.0‰, -5.1‰ and -5.0‰, respectively, as well as abrupt drop in carbonate content in sample 19 into 38.5% (Fig. 4).

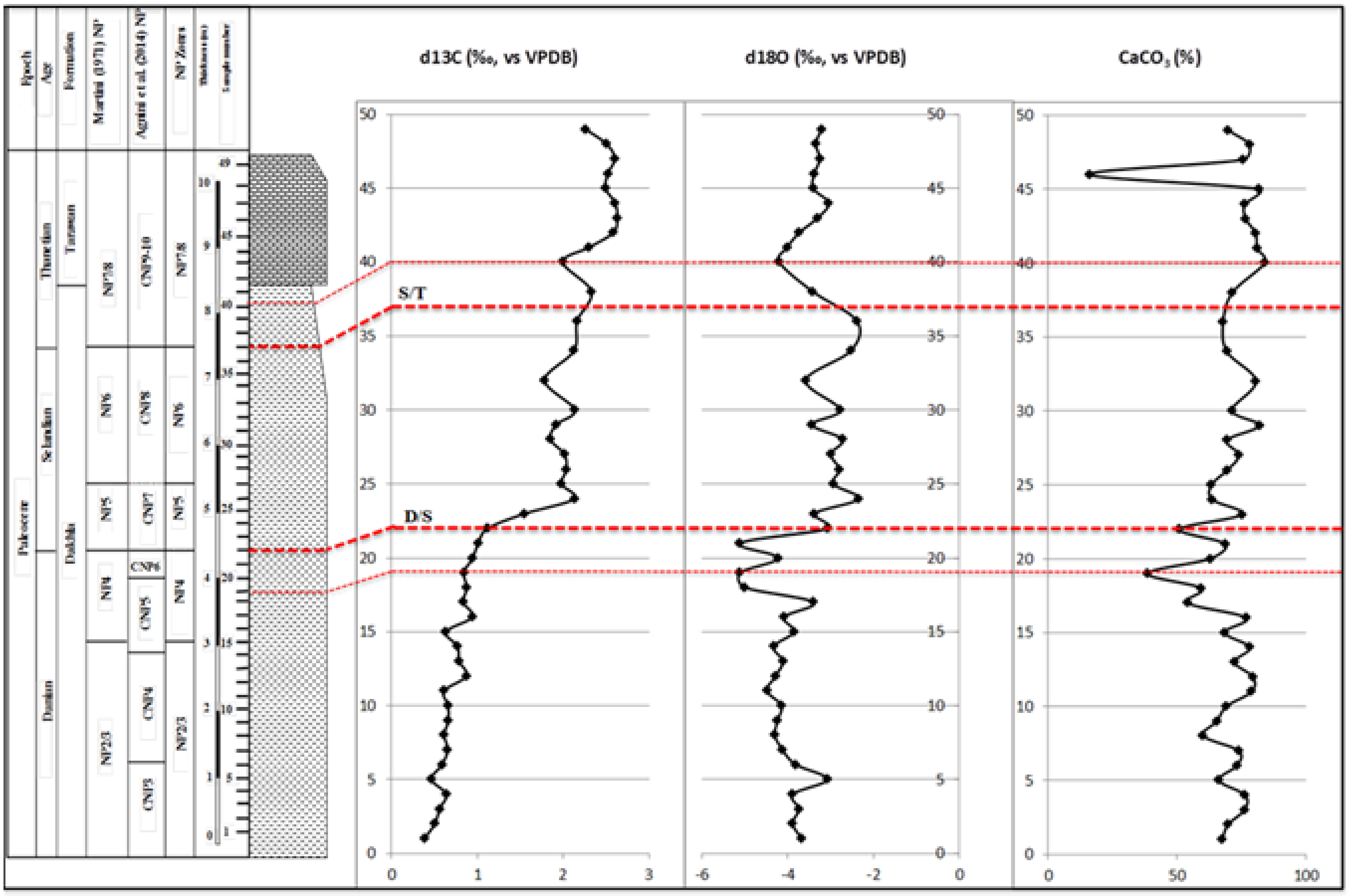

Fig. 4: Data of $\delta^{13}C$, $\delta^{18}O$ and carbonate contents of the study interval at Nukhul, Sinai, Egypt.

6. Remarks and Discussion

Variations in calcareous nannofossil assemblages, $\delta^{18}O$ and $\delta^{13}C$ values as well as changes in $CaCo_3$ contents are helpful tools for precise delineation of the stages boundaries of Paleocene (Kasem et al., 2017). A distinct bed within the Dakhla F. often marks the Late Danian Event (LDE) in Egypt (Bornemann et al., 2009; Sprong et al., 2011, 2013, and Monechi et al., 2013). However, this bed was not recorded at Nukhul (Fig. 3). The base of LDE was placed in between the LO of *C. edentulus* to the LCtO of *S. primus* (Kasem et al., 2017). At Nukhul, *C. edentulous* appears for the first time in sample 20 coincident with the LO and LCtO of *S. primus* (Table). The LDE was placed at sample 19 as indicated by sudden drop in carbonate content from 59.5% in sample 18 to 38.5% in sample 19. Moreover, $\delta^{18}O$ values suddenly decreases from -3.4‰ in sample 17 to 5.0 ‰ and 5.1‰ in samples number 18 and 19, respectively, (Fig. 4). No remarkable variations in $\delta^{13}C$ values were noted across this interval. An increase in the frequency of *Prinsius* in the LDE interval was noted (Monechi et al., 2013); yet, this notice was not documented in the study section. Calcareous nannofossil's abundance and species richness have minimum values in sample 19 (Table and figure 5) indicating dissolution of calcareous fossils.

The recognition of the base of Selandian is commonly problematic as a consequence of the rarity or absence of the bioevents adopted in biozonation for this period (Sprong et al., 2009). In Egypt, the D/S boundary had been delineated within Zone NP4 at the LO of genus

Fasciculithus, at the LO of *Diantholitha mariposa*, within Subzone NTp8c; at the LOs of *Fasciculithus* sp. plus *Sphenolithus primus*, at the topmost of a considerable drop in the carbon isotope, or at NP5 Zone's base (Faris et al., 1999a, b; Tantawy et al., 2000; Faris et al., 2005a, b; Faris and Abu Shama, 2007; Faris and Salem, 2007; Youssef, 2009; Aubry and Salem, 2013a). Moreover, a proposition it had been suggested to delineate the contact between the Danian and Selandian by the LO and diversification of the *Diantholitha* and *Lithoptychius* (Aubry and Salem, 2013b).

In 2005, Clemmensen and Thomsen placed the Selandian's base at its type locality in Denmark at the NP4/NP5 zonal boundary that coincides the change in lithology from the Danian limestones to the Selandian Green sand. At the GSSP Zumaia section, this boundary was marked by the ending of flourish of *Braarudosphaera bigelowii* near the top of Zone NP4 (Schmitz et al., 2011). It occurs above or almost at a level coincides with the second radiative episode of fasciculiths and the variation from the Aitzgorri Limestone F. to the marly Itzurun F. (Schmittz et al., 1998; Bernaola et al., 2007, 2009, and Schmitz et al., 2011). However, the End Acme of *Braarudosphaera bigelowii* is restrictive to the north Atlantic, the North Sea Basin and Zumaia, and cannot be applied to the Tethyan areas (Schmitz et al., 2011). In this study, *B. bigelowii* is *sporadic*, however, it occurs with common abundance in sample 17 (Table).

Furthermore, the 2nd radiation of genus fasciculiths was delineated by *the LO of Lithoptychius ulii* (Schmitz et al., 2011). Because *L. ulii* first occurs slightly beneath the D/S boundary and *F. tympaniformis* occurs above *it* at Zumaia (Schmitz et al., 2011), the D/S boundary can be approximated within the interval between these two bioevents at the Tethyan area (Kasem et al., 2017). At Nukhul, the LOs of *L. ulii* and *F. tympaniformis* are synchronized and, therefore, the D/S boundary was placed at the base of calcareous nannofossil Zone NP5 (sample 22). No lithological variation was noted across this boundary (Fig. 3). Moreover, no remarkable changes in $\delta^{13}C$ and $\delta^{18}O$ data were recorded close to NP4/NP5 zonal boundary except the increase in $\delta^{13}C$ values in samples 23 and 24 slightly above this boundary and the sudden drop in $\delta^{18}O$ values just below this boundary in sample 21 (Fig. 3). Furthermore, the calcium carbonate contents show a remarkable decrease from 69.0% in sample 21 to 51.0 % in sample 22 (Fig. 4). The absence of representatives of the first radiation of fasciculiths (*Diantholitha* sp., *Lithoptychius varolii*, and *L. chowii*), co-occurrence of the LOs of *S. primus* and *C. edentulous*, coincidence of the LOs of *L. ulii* and *Fasciculithus tympaniformis*, *L. janii*, *L. stegastus*, *F. clinatus* and *Bomolithus elegans* (Table) indicates a hiatus within the Danian interval at Nukhul.

The abundance of calcareous nannofossil decreases in sample 21 and 22 into 1 and 2.7 specimen per field of view (S/FOV), respectively; whereas diversity decreases into 13 species in sample 21 (Table and figure 5). These variations reflect dissolution of carbonates during this interval.

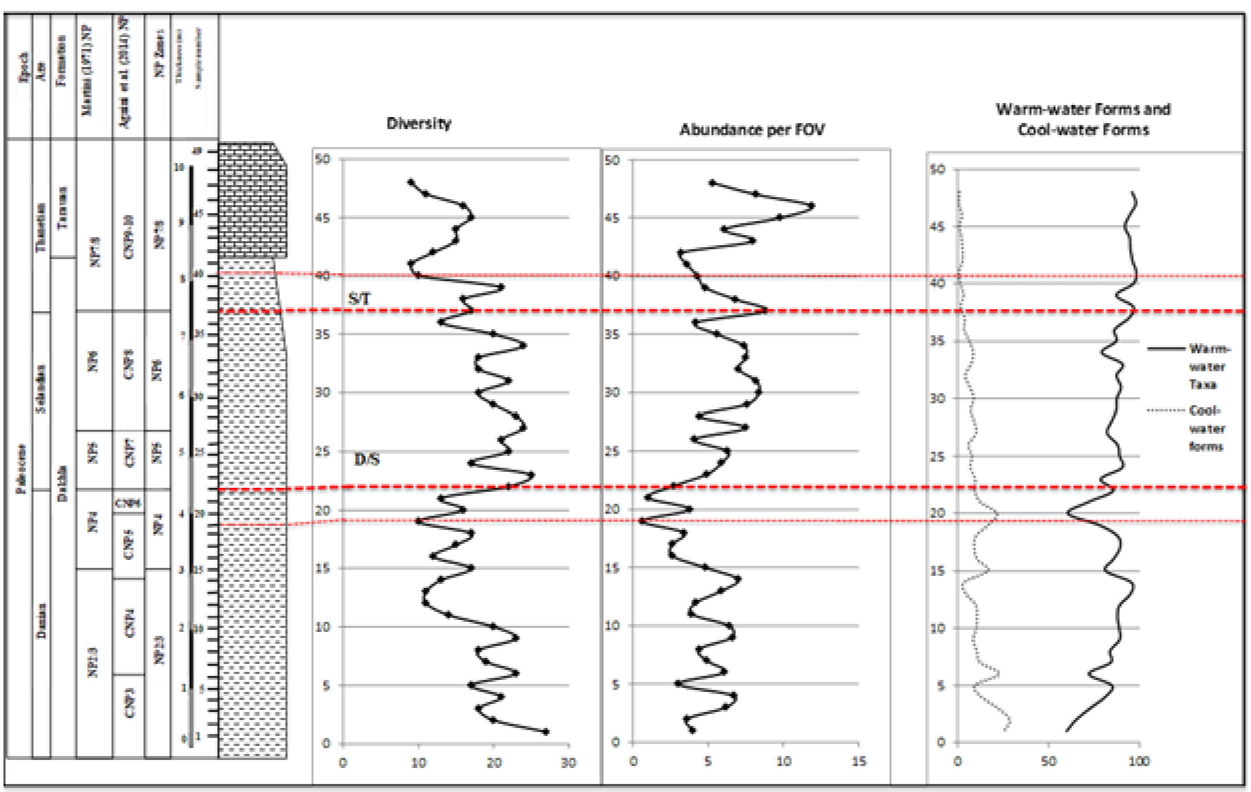

Fig. 5: Calcareous nannofossil abundance, diversity, and counts of warm-water taxa relative to cool-water taxa.

Thanetian Stage's base at Zumaia was delineated at the start of magnetochron C26n without any characteristic variation in lithology, assemblages of planktonic foraminifera, or in the $\delta^{13}C$ values across the S/T transition (Schmitz et al., 2011).

The most important event for approximating the S/T boundary is the MPBE that is a global short-lived biotic event and possibly related to warming episode (Schmitz et al., 2011). It occurs at about 2.8 m beneath the base of the Thanetian and about 4.5 m overhead of the onset of Zone NP6 (Schmitz et al., 2011). The MPBE at Zumaia is delineated by a remarkable falling in the content of carbonate and $\delta^{13}C$ (Bernaola et al., 2007).

The S/T boundary was delineated in Egypt at the start of Zone NP7/8 (Faris and Farouk, 2012) at the contact between the Dakhla F. and the Tarawan F. and, therefore, a hiatus was suggested at this boundary as it is evident by the change in lithology from Dakhla Shale to the limestones of the Tarawan F. (e. g. Kasem et al 2017). Discrepancies in calcareous nannofossils age dating of the start of Tarawan F. were attributed to variations in relative water depths during deposition at various localities (Aubry and Salem 2013b). These variations are likely attributed to tectonics that resulted in uplift and subsidence in various areas, and therefore, affect water depth (Paleobathymetry) and the diversity of nannofossils.

The S/T boundary at Nukhul was approximated at the start of Zone NP7/8 within the upper part of Dakhla F. without any significant lithological change (Fig. 3). At Nukhul, no considerable variations in the calcareous nannofossils were recorded through this interval excepting the LO of *D*. *mohleri* (Table) and the Dakhla F. is conformably overlain by the Tarawan F., where calcareous nannofossil Zone NP7/8 extends throughout these formations (Fig. 3).

No characteristic variations in $\delta^{13}C$ and $\delta^{18}O$ values were noted within Zone NP6 or close to the NP7/8 Zone's base except the sudden drop in sample 32 below it and sample 40 above it (figure 4). The $\delta^{13}C$ values drops from 2.2 ‰ in sample 30 to 1.8‰ in sample 32 and drops from 2.3 ‰ in sample 38 to 2.0 in sample 40 (figure 3). Similarly, The $\delta^{18}O$ values drops from -2.8 ‰ in sample 30 to -3.8 ‰ in sample 32 and drops from -2.4 ‰ in sample 36 to -4.2 in sample 40 (figure 3).

The diversity decreases into 13 species in sample 36 and drops into 9 species in sample 41 (Table and figure 5). Similarly, the abundance decreases into 4.2 S/FOV in sample 36 and drops into 3.2 S/FOV in sample 42 (Table and Fig. 4).

Previous studies recognized the ecological preferences of certain taxa (see Kasem et al., 2022 for references). Based on these studies, the warm-water taxa recognized in the present study include: *Thoracosphaera operculata*, *T. saxea*, *Coccolithus pelagicus*, *Ericsonia subpertusa*, *Zygrhablithus bijugatus*, *Fasciculithus* spp., *Sphenolithus* spp., *Rhomboaster* spp., *Tribrachiatus* spp., *Pontosphaera* spp.; *Discoaster* spp., *Heliolithus kleinpellii*, and *Bomolithus* spp.; whereas, the cool-water taxa include *Zeugrhabdotus sigmoides*, *Markalius inversus*, *Cruciplacolithus* spp., *Prinsius* spp., *Chiasmolithus* spp., *Neochiastozygus junctus*, *Blackites* spp., *Neococolithus protens, Toweius eminens*, and *T. tovae* (figure 5). The abundance of warm-water forms comparable to the cold-water taxa shows upward increase in water temperature and oligotrophic conditions during the Paleocene interval (Fig. 5).

Several evidences support tectonic disturbance in the study area. These supports include: 1) the presence of hiatuses and the absence of some calcareous nannofossil zones within the Danian stage; 2) the noticed variations of $\delta^{13}C$ and $\delta^{18}O$, and carbonate contents as well as calcareous nannofossil diversity at the boundaries. 3) the partial absence of distinctive beds within the Dakhla Formation that mark the Late Danian Event at this locality; and (4) The abrupt transition from siliciclastics (Dakhla Fm) to dominant carbonates (Tarawan Fm) (Prof. ? personal communication).

7. Summary and conclusion

Variations in calcareous nannoplankton assemblages, $\delta^{13}C$ as well as $\delta^{18}O$ values plus carbonate contents were tracked at the Nukhul section, Sinai, Egypt. The study interval that outcrops at Nukhul covers the Dakhla - Tarawan formations. Five calcareous nannofossil zones were recognized that are NP2/3, NP4, NP5, NP6, and NP7/8. The LDE was placed based on sudden decrease in carbonate contents and $\delta^{18}O$ values, however, no distinct changes in $\delta^{13}C$ values were recorded throughout this interval. The diversity and abundance of calcareous nannofossils reach their minimum values at this level as a result of dissolution carbonates. The Selandian's base was tentatively delineated at NP5 Zone's base without any lithological change across this boundary. No distinct changes in $\delta^{13}C$ and $\delta^{18}O$ values were documented close to this level except the abrupt decrease in $\delta^{18}O$ values just below this boundary and increase in $\delta^{13}C$ values slightly above it. The calcium carbonate contents show a distinct drop close to this level. The diversity and abundance of calcareous nannofossil show remarkable decreases around the NP4/NP5 zonal boundary reflecting a dissolution episode of carbonates. The absence of *Diantholitha* sp*.,* early representatives of *Lithoptychius*, coincidence of the LOs of *S. primus* and *C. edentulous*, and the LOs of *L. ulii* and *Fasciculithus tympaniformis*, *L. janii*, *L. stegastus*, *F. clinatus* and *Bomolithus elegans* indicate a hiatus within the Danian interval at the Nukhul section. Thanetian's base was delineated at the top of Zone NP6 within the upper part of Dakhla F. without any significant change in lithology or in the nannofossil assemblages except the LO of *D*. *mohleri*. Calcareous nannofossil Zone NP7/8 extends from the Dakhla F. to the Tarawan F. indicating conformable relationship between them at Nukhul. No remarkable change in $\delta^{13}C$ and $\delta^{18}O$ values were recorded at or around the base of Zone NP7/8 except the abrupt decreases in sample 32 below and sample 40 above this boundary. Fluctuations in diversity and abundances were documented close to NP7/8 Zone's base at the study section. Ecological preferences of calcareous nannofossil assemblages in study section reveal an upward increase in paleotemperature of water throughout the Paleocene. The Paleocene sediments exposed at Nukhul area is a good section for tracking the variations in calcareous nannofossils and sedimentary with changes in the paleoclimate.

Acknowledgments: I express my deepest appreciation to Prof. Sherwood Wise (Florida State University, USA) for helping me during the examination of this section

Appendix A. Supplementary data

Supplementary data to this article can be found online at 10.21608/FSRT.2023.178854.1078

References

Abu Shama A.M., Wanas H.A., and El-Nahrawy S.A. Calcareous Nannofossil Biostratigraphy of the Paleocene-Lower Eocene Successions in the Farafra Oasis, Western Desert, Egypt. Journal of African Earth Sciences, V. 150, 2019, P. 466-484*. DOI:* 10.1016/j.jafrearsci.2018.09.021.

Agnini, C, Fornaciari E, Raffi I, Rio D, Röhl U, Westerhold T (2007). High-resolution nannofossil biochronology of middle Paleocene to early Eocene at ODP Site 1262: implications for calcareous nannoplankton evolution. Marine Micropaleontology, 64 (2007), p. 215-248.

Agnini C, Fornaciari E, Raffi I, Catanzariti R, Pälike H, Backman J, Rio D (2014). Biozonation and biochronology of Paleogene calcareous nannofossils from low and middle latitudes. Newsletters on stratigraphy, V. 47/2 (2014), pp. 131-181.

Agnini C, Monechi, S. and Raffi I. (2017). Calcareous nannofossil biostratigraphy: historical background and application in Cenozoic chronostratigraphy. Lethaia, V. 50, pp. 447–463.

Arenillas I, Molina E, Ortiz S, Schmitz B (2008). Foraminiferal and $\delta^{13}C$ isotopic event-stratigraphy across the Danian–Selandian transition at Zumaya (northern Spain): chronostratigraphic implications. Terra Nova, 20 (2008), pp. 38–40.

Aubry M-P, Salem R (2013a). The Dababiya Quarry Core: Coccolith Biostratigraphy. Stratigraphy, V. 9 (2012) (2013), pp. 241–259.

Aubry M-P, Salem, R (2013b). The Dababiya Core: a window into Paleocene to Early Eocene depositional history in Egypt based on coccolith stratigraphy. Stratigraphy V. 9 (2012) (2013), pp. 287–346.

Aubry, M.-P., Ouda, K., Dupuis, C., Berggren, W.A., Van Couvering, J.A., Members of the Working Group on the Paleocene/Eocene Boundary (2007). The Global Standard Stratotype-Section and Point (GSSP) for the base of the Eocene Series in the Dababiya section (Egypt). Episodes, 30 (4) (2007), pp. 271–286.

Aubry, M.-P. (1998). Early Paleogene calcareous nannoplankton evolution: a tale of climatic amelioration. In: Aubry, M.-P., Ouda, K. (Eds.), Late Paleocene–early Eocene Biotic and Climatic Events in the Marine and Terrestrial Record Columbia University Press, New York, pp. 158–201.

Awad GH, Ghobrial MG (1965). Zonal Stratigraphy of the Kharga Oasis. Ministry of Industry, General Egyptian Organization for Geological Research and Mining, Geological Survey, Cairo, paper no. 34, pp. 1-77.

Bernaola G, Baceta JI, Orue-Extebarria X, Alegret L, Martin-Rubio M, Arostegui J, Dinarès-Turell J (2007). Evidence of an abrupt environmental disruption during the mid-Paleocene biotic event (Zumaia section, western Pyrenees). Geological Society of America Bulletin, 119 (2007), pp. 785–795.

Bernaola G, Martín-Rubio M, Baceta JI (2009). New high resolution calcareous nannofossil analysis across the Danian/Selandian transition at the Zumaia section: comparison with South Tethys and Danish sections. Geologica Acta, 7 (2009), pp. 79–92.

Bornemann, A. (2003). Case studies of Mesozoic calcareous nannofossils: Implications for paleoecology, calcareous nannofossil morphology and carbonate accumulation. PhD Thesis, Ruhr-University, Bochum, 2003, 126 pp.

Bornemann, A., Schulte, P., Sprong, J., Steurbaut, E., Youssef, M., and Speijer, R.P. (2009). Latest Danian carbon isotope anomaly and associated environmental change in the Southern Tethys (Nile Basin, Egypt). Journal of the Geological Society of London, 166 (2009), pp. 1135–1142.

Bown, P.R., Lees, J.A., and Young, J.R. (2004). Calcareous nannoplankton evolution and diversity through time. In: H.R. Thierstein, J.R. Young (Eds.), Coccolithophores, From Molecular Processes to Global Impact Springer Verlag, Berlin, Germany (2004), pp. 481–508.

Brotzen, F., 1959. On Tylocidaris species (Echinoidea) and the stratigraphy of the Danian of Sweden. With a bibliography of the Danian and Paleocene. Sveriges Geologiska Undersokning, Arsbok, 54(2), p. 1-81.

Bukry D (1973). Low-latitude coccolith biostratigraphic zonation. Initial Reports of Deep Sea Drilling Project, vol. 15(1973), U.S. Government Printing Office, Washington, pp. 685-703.

Clemmensen A, Thomsen E (2005). Palaeoenvironmental changes across the Danian–Selandian boundary in the North Sea Basin. Paleogeography, Paleoclimatology and Paleoecology, 219 (2005), pp. 351–394.

Coccioni R, Frontalini F, Bancalà G, Fornaciari E, Jovane L, Sprovieri M (2010). The Dan-C2 hyperthermal event at Gubbio (Italy): global implications, environmental effects, and cause(s). Earth and Planetary Science Letters, 297 (2010), pp. 298–305.

Coplen, T. B., 1996. More uncertainty than necessary, Paleoceanography, 11 (1996), pp. 369-370.

Dickens, G.R., Castillo, M.M., and Walker, J.C.G., 1997. A blast of gas in the latest Paleocene: simulating first-order effects of massive dissociation of oceanic methane hydrate. Geology, 25 (3) (1997), pp. 259–262.

Dinarès-Turell, J., Pujalte, V., Stoykova, K., Baceta, J.I., and Ivanov, M., 2012. The Palaeocene "top chron C27n" transient greenhouse episode: evidence from marine pelagic Atlantic and peri-Tethyan sections. Terra Nova, 24 (2012), pp. 477–486.

Dupuis C, Aubry M-P, Steurbaut E, Berggren WA, Ouda K, Magioncalda R, Cramer BS, Kent DV, Speijer RP, Heilmann-Clausen C (2003). The Dababiya Quarry section: lithostratigraphy, clay mineralogy, geochemistry and paleontology. Micropaleontology, V. 49 (2003), pp. 41–59.

Erba, E., Castradori, F., Guasti, G., and Ripepe, M., 1992. Calcareous nannofossils and Milankovitch cycles: the example of the Gault Clay Formation (southern England). Paleogeography, Paleoclimatology and Paleoecology, 93 (1992), pp. 47–69.

Eshet, Y., Moshkovitz, S., Habib, D., Benjamini, C., and Margaritz, M., 1992. Calcareous nannofossil and dinoflagellate stratigraphy across the Cretaceous/Tertiary boundary at Hor Hahar, Israel. Marine Micropaleontology, 18 (1992), pp. 199–228.

Faris, M., and Abu Shama, A. M., 2007. Nannofossil biostratigraphy of the Paleocene lower Eocene succession in the Thamad area, east central Sinai, Egypt. Micropaleontology, 53 (1–2) (2007), pp. 127–144.

Faris M, Farouk S (2012). Integrated biostratigraphy of two Upper Maastrichtian-Paleocene successions in north-central Sinai, Egypt. Geologia Croatica, pp. 139-160, 65/2, Zagreb, 2012.

Faris M, Salem R (2007). Paleocene-Eocene calcareous nannofossil biostratigraphy in west central Sinai, Egypt. Proceeding of the 8th Conference on Geology of Sinai for Development, Ismailia, 2007, pp. 1-14.

Faris M, Abdel Hameed AT, Shaaban M (1999). Calcareous nannofossil events at the Cretaceous/Paleocene boundary in central Egypt. The 1st international conference on the Geology of Africa, V. 2 (1999), p. 21-42, Assiut, Egypt.

Faris M, Ayyad SN, El-Nahass HA, Al Wosabi, KA (2005). Early Paleogene stages and their boundaries, Sinai, Egypt. In: 4th international conference on the Geology of Africa, Assiut Univ., Egypt, V. (2), pp. 753–768.

Faris M., Obaidalla, N. A. Metwally A. A, Salman A. M. and Zaky A. S. (2018). Late Cretaceous–Early Paleogene tectonic events at Farafra-Abu Minqar Stretch, Western Desert, Egypt: results from calcareous plankton. Arabian Journal of Geosciences, volume 11: 429 (2018).

Guiraud R., and Bosworth W., 1999. Phanerozoic geodynamic evolution of northeastern Africa and the northwestern Arabian platform. Tectonophysics, 315 (1999), pp. 73–108.

Haq, B.U., and Lohmann, G.P., 1976. Early Cenozoic calcareous nannoplankton biogeography of the Atlantic Ocean. Marine Micropaleontology, 1 (1976), pp. 119–194.

Haq, B.U., Premoli Silva, I., and Lohmann, G.P. 1977. Calcareous plankton paleobiogeographic evidence for major climatic fluctuations in the Early Cenozoic Atlantic Ocean. Journal of Geophysical Research, 82 (1977), pp. 3861–3876.

Hay, W.W., 1964. The Use of the Electron Microscope in the Study of Fossils. Smithsonian Institution Annual Reports, 1963, pp. 409-415.

Hay, W.W., and Mohler, H.P., 1967. Calcareous nannoplankton from early Tertiary rocks at Pont Labau, France, and Paleocene–early Eocene correlations. J. Paleontol. 41 (6), pp. 1505–1541.

Jenkins DG, Luterbacber HP (1992) Paleogene Stages and their boundaries. Neues Jahrbuch für Geologie und Paläontologie abhandlungen, 186, pp. 1-5.

Karoui-Yaakoub, N., Mtimet M. S., Grira C., Guesmi W., and Bejaoui S. (2016). Planktonic foraminiferal biostratigraphy and paleoenvironment of the Danian/Selandian in west-central Sinai (Egypt), implications from the Nukhul section. Arabian Journal of Geosciences volume 9, Article number: 487 (2016)

Kasem, A., M., Wise, Jr., Faris, M., Farouk, S., Zahran, E., 2017. Calcareous nannofossil biostratigraphy of the Paleocene at the Misheiti section, East Central Sinai, Egypt. Arabian Journal of Geosciences (2017): 10-455. DOI 10.1007/s12517-017-3217-4.

Kasem, A., M., Faris, M., Jovane L., Ads T., A., Frontalini, F., Zaky A. S., 2022. Biostratigraphy and Paleoenvironmental Reconstruction at the Gebel Nezzazat (Central Sinai, Egypt): A Paleocene Record for the Southern Tethys (2022). Geosciences 2022, 12, 96. https://doi.org/10.3390/geosciences12020096.

Martini E (1971). Standard Tertiary and Quaternary calcareous nannoplankton zonation. In: Farinacci, A. (Eds.), Proceedings of the II Planktonic Conference 2, Roma (1970), pp. 739–785.

Monechi S, Reale V, Bernaola G, Balestra B (2013). The Danian/Selandian boundary at Site 1262 (South Atlantic) and in the Tethyan region: biomagnetostratigraphy, evolutionary trends in fasciculiths and environmental effects of the Latest Danian Event. Marine Micropaleontology, 98 (2013), pp. 28–40.

Okada H, Bukry D (1980). Supplementary modification and introduction of code numbers to the low-latitude coccolith biostratigraphic zonation (Bukry, 1973; 1975). Marine Micropaleontology 5 (1980), pp. 321–325.

Perch-Nielsen K (1985). Cenozoic calcareous nannofossils. H.M. Bolli, J.B. Saunders, K. Perch-Nielsen (Eds.), Plankton Stratigraphy, Cambridge University Press, Cambridge (1985), pp. 427–554.

Quillévéré F, Aubry M-P, Norris RD, Berggren WA (2002). Paleocene oceanography of the eastern subtropical Indian Ocean: an integrated magnetobiostratigraphic and stable isotope study of ODP Hole 761B (Wombat Plateau). Paleogeography, Paleoclimatology and Paleoecology, 184 (3–4) (2002), pp. 371–405.

Quillévéré F, Norris RD, Kroon D, Wilson PA (2008). Transient Ocean warming and shifts in carbon reservoirs during the early Danian. Earth and Planetary Science Letters, 265 (2008), pp. 600–615

Romein AJT (1979). Lineages in Early Paleocene nannoplankton. Utrecht Micropaleontology Bulletin, 22 (1979), pp. 18–22.

Said, R., 1961. Tectonic framework of Egypt and its influence on distribution of foraminifera. Am. Assoc. Petroleum Geologists Bull., 45 (1961), p. 198–218.

Schmitz B, Molina E, von Salis K (1998). The Zumaya section in Spain; a possible global stratotype section for the Selandian and Thanetian stages. Newsletters on Stratigraphy, 36 (1998), pp. 35–42.

Schmitz B, Pujalte V, Molina E et al (2011). The Global Stratotype Sections and Points for the bases of the Selandian (Middle Paleocene) and Thanetian (Upper Paleocene) stages at Zumaia, Spain. Episodes, 34 (2011), pp. 220–243.

Shaaban, M.N., 1997. Stable Isotops Stratigraphy across the K/T Boundary, and Isotopic Investigations of an “Ignored” Worm Bed, Eastern Desert, Egypt. Facies, 37, pp. 137-146, Erlangen, 1997.

Soliman MF, Obaidalla, NA, Ahmed E. A. and Kurzweil J. (2014). Mid-Paleocene event at Gabal Nezzazat, Sinai, Egypt: planktonic foraminiferal biostratigraphy, mineralogy and geochemistry. Arabian Journal of Geosciences 7(10):4079-4099. DOI: 10.1007/s12517-013-1066-3

Speijer RP (2003a). Systematics and paleoecology of the foraminifer Neoeponides duwi (Nakkady) from the Paleocene of Egypt. Micropaleontology, 49 (2003), pp. 146–150.

Speijer RP (2003b). Danian–Selandian sea-level change and biotic excursion on the southern Tethyan margin, in: S.L. Wing, P.D. Gingerich, B. Schmitz, E. Thomas (Eds.), Causes and consequences of globally warm climates in the Early Paleogene, Geological Society of America Special Paper 369 (2003), p. 275–290.

Sprong J, Speijer RP, Steurbaut E (2009). Biostratigraphy of the Danian/Selandian transition in the southern Tethys. Special reference to the lowest occurrence of planktic foraminifera Igorina albeari. Geologica Acta, 7 (2009), pp. 63–77.

Sprong J, Youssef M, Bornemann A, Schulte P, Stassen P, Steurbaut E, Kouwenhovens TJ, Speijer RP (2011). A multi-proxy record of the Latest Danian Event at Gebel Qreiya, Eastern Desert, Egypt. Journal of Micropalaeontology, 30 (2011), pp. 167–182.

Sprong J, Kouwenhoven TJ, Bornemann A, Schulte P, Stassen P, Steurbaut E, Youssef M, Speijer RP (2012). Characterization of the Latest Danian Event by means of benthic foraminiferal assemblages along a depth transect at the southern Tethyan margin (Nile Basin, Egypt). Marine Micropaleontology, 86–87 (2012), pp. 15–31.

Sprong J, Kouwenhovens TJ, Bornemann A, Dupuis C, Speijer RP, Stassen P, Steurbaut E (2013). In search of the Latest Danian Event in a paleobathymetric transect off Kasserine Island, north-central Tunisia. Paleogeography, Paleoclimatology and Paleoecology, V. 379-380 (2013), pp. 1-16.

Stassen, P., Dupuis, C., Morsi, A.M., Steurbaut, E., and Speijer, R.P., 2009. Reconstruction of a latest Paleocene shallow-marine eutrophic paleoenvironment at Sidi Nasseur (Central Tunisia) based on foraminifera, ostracoda, calcareous nannofossils and stable isotopes ($\delta^{13}C$, $\delta^{18}O$). Geologica Acta, 7 (2009), pp. 93–112.

Tantawy AA (1998). Stratigraphical and Paleoecological Studies on Some Paleocene–Eocene Successions in Egypt. Unpub. Ph.D. Thesis, Aswan Faculty of Science, South Valley Univ., Egypt, 273 p.

Tantawy AA, Ouda K, Von Salis K, Saad El Din M (2000). Biostratigraphy of Paleocene sections. In: Schmitz, B., Sundquist, B., Andreasson, F. (Eds.), Early Paleogene Warm Climates and Biosphere Dynamics, GFF, vol. 122, pp. 163–165.

Thierstein, H.R., 1980. Selective dissolution of Late Cretaceous and Earliest Tertiary calcareous nannofossils: experimental evidence. Cretaceous Research, 2 (1980), pp. 165–176.

Thierstein, H.R., and Haq, B.U., 1977. Maestrichtian/Danian biogeographic variations in calcareous nannoplankton (abstract). J. Paleontol., 51 (1977), pp. 28.

Thomas D.J., Bralower T.J., and Zachos J.C., 1999. New evidence for subtropical warming during the late Paleocene thermal maximum: stable isotopes from Deep Sea Drilling Project Site 527, Walvis Ridge. Paleoceanography, 14 (1999), pp. 561–570.

Van Heck SE, Prins B (1987) A refined nannoplankton zonation for the Danian of the Central North Sea. International Nannoplankton Association, Vienna Meeting, V. 39 (1987), pp. 285–303.

Varol O (1989). Palaeocene calcareous nannofossil biostratigraphy. In: J.A. Crux, S.E. Van Heck (Eds.), Nannofossils and Their Applications, British Micropaleontological Society. Ser, 12 (1989), pp. 267–310.

Wei, W., and Wise, S.W.Jr., 1990. Biogeographic gradients of middle Eocene-Oligocene calcareous nannoplankton in the South Atlantic Ocean. Palaeogeography Palaeoclimatology Palaeoecology 79, pp. 29–61.

Westerhold, T., Röhl, U., Raffi, I., Fornaciari, E., Monechi, S., Reale, V., Bowles, J., and Evans, H.F., 2008. Astronomical calibration of the Paleocene Time. Palaeogeography, Palaeoclimatology, Palaeoecology, 257 (2008), pp. 377–403.

Westerhold, T., Röhl, U., Donner, B., McCarren, H.K., and Zachos, J., 2011. A complete high-resolution Paleocene benthic stable isotope record for the central Pacific (ODP Site 1209). Paleoceanography, 26 (2011), p. PA2216.

Wind, F.H., 1979. Maestrichtian–Campanian nannofloral provinces of the southern Atlantic and Indian Oceans. In: Talwani, M., et al. (Eds.), Deep Drilling Results in the Atlantic Ocean: Continental Margins and Paleoenvironment. Washington, American Geolphysical Union, pp. 3, pp. 123–137.

Youssef M (2009). High resolution calcareous nannofossil biostratigraphy and paleoecology across the Latest Danian Event (LDE) in central Eastern Desert, Egypt. Marine Micropaleontology, 72 (2009), p. 111–128.

Zachos, J.C., Röhl, U., Schellenberg, S.A., Sluijs, A., Hodell, D.A., Kelly, D.C., Thomas, E., Nicolo, M., Raffi, I., Lourens, L.J., McCarren, H., and Kroon, D., 2005. Rapid acidification of the ocean during the Paleocene–Eocene Thermal Maximum Science, 308 (2005), pp. 1611–1615.